

Research Article

Cite this article: Seto N, Kashiyama K (2020). Astrometric study of Gaia DR2 stars for interstellar communication. *International Journal of Astrobiology* **19**, 308–313. <https://doi.org/10.1017/S147355042000004X>

Received: 24 January 2020
Revised: 5 March 2020
Accepted: 14 March 2020
First published online: 17 April 2020

Keywords:

Extraterrestrial intelligence; astrobiology

Author for correspondence:

Naoki Seto,
E-mail: seto@tap.scphys.kyoto-u.ac.jp

¹Department of Physics, Kyoto University, Kyoto 606-8502, Japan; ²Research Center for the Early Universe, Graduate School of Science, University of Tokyo, Bunkyo-ku, Tokyo 113-0033, Japan and ³Department of Physics, Graduate School of Science, University of Tokyo, Bunkyo-ku, Tokyo 113-0033, Japan

Abstract

We discuss the prospects of high precision pointing of our transmitter to habitable planets around Galactic main sequence stars. For an efficient signal delivery, the future sky positions of the host stars should be appropriately extrapolated with accuracy better than the beam opening angle Θ of the transmitter. Using the latest data release (DR2) of Gaia, we estimate the accuracy of the extrapolations individually for 4.7×10^7 FGK stars, and find that the total number of targets could be $\sim 10^7$ for the accuracy goal better than $1''$. Considering the pairwise nature of communication, our study would be instructive also for SETI (Search for Extraterrestrial Intelligence), not only for sending signals outward.

Introduction

Even ~ 60 years have passed since the pioneering work by Drake, we have not succeeded to detect a convincing signature of extraterrestrial intelligence (ETI) (e.g. Drake 1961; Horowitz and Sagan 1993; Tarter 2001; Siemion *et al.* 2013). On one hand, this might be simply reflecting the possibility that the number of Galactic civilizations is small, or even zero on our past light-cone. On the other hand, our observational facilities and available computational resources might not be sufficient to deal with existing weak signals in a huge parameter space (Tarter *et al.* 2010; Wright *et al.* 2018). In any case, SETI programmes are actively ongoing, including recently launched Breakthrough Listen in which $\sim 10^6$ Galactic stars and $\sim 10^2$ nearby galaxies will be analysed (Gajjar *et al.* 2019).

In parallel with the searching efforts, artificial signals have been intentionally transmitted from the Earth to extraterrestrial systems (e.g. Zaitsev 2010, see also Baum *et al.* 2011; Vakoch 2016). For example, Polaris has been repeatedly selected as a target. In 2008, a 70 m-dish antenna of NASA's Deep Sky Network was used for a radio transmission in the X-band (wavelength $\lambda \sim 4$ cm). More recently, in 2016, an ESA's antenna (dish size $L = 35$ m) was directed to Polaris for sending messages encoded in $\lambda \sim 4$ cm radio waves. Here we should comment that the 1–10 GHz band (wavelength 3–30 cm) is regarded as an ideal window for interstellar communication, given the background noises (Cocconi and Morrison 1959). The half opening angle of the transmitted beam is given by $\Theta \sim \lambda/(2L)$, and we have $O(100'')$ for the two concrete cases mentioned above.

Considering the potential limitations of observational facilities and computational resources inversely at ETI side, it would be more advantageous to increase the energy flux of our outgoing signals. Here one of the solid options is to reduce the beam opening angle Θ (e.g. Benford *et al.* 2010, see also Hippke 2019). For example, using a phased array with an effective diameter comparable to the core station of SKA2, we can realize $\Theta \sim 0.8''(\lambda/4 \text{ cm})(L/5 \text{ km})^{-1}$. Note that, for a given beam opening angle Θ , the size of the transmitter L could be reduced by using a shorter wavelength λ . Clark and Cahoy (2018) studied intentional signal transmissions in the optical/IR bands for which typical seeing level on the surface of the earth is $O(1'')$. Even though the Sun becomes a much stronger background than in the radio band, they discussed that a facility similar to the Airborne Laser ($L = 1.5$ m, $\lambda = 1315$ nm, $\Theta \sim 0.1''$) could be workable, depending on the size of the receiver's telescope. Meanwhile, the lightsail propulsion has been studied as an attractive technology for future interplanetary and interstellar missions. Under certain restrictions, Guillochon and Loeb (2015) showed an optimal combination $L = 1.5$ km and $\lambda = 0.4$ cm for interplanetary transportations, corresponding to $\Theta \sim 0.3''$. With a potential light beamer ($L \sim 1$ km, $\lambda \sim 1 \mu\text{m}$) for the Breakthrough Starshot, the diffraction would be $O(0.001'')$.¹

However, a target star is moving on the sky with proper motion μ , and there is an offset angle between its observed position and the appropriate transmission direction. Given the round-trip time $2d/c$ (d : the target distance) of photon, the offset is estimated to be

¹<https://breakthroughinitiatives.org/forum/28?page=4>

$2d/c \times \mu = 2(v_t/c) = 40''(v_t/30 \text{ km s}^{-1})$ with the transverse velocity v_t (Zaitsev 2010; Arnold 2013). Therefore, if we use a beam $\Theta \leq 40''$ and want to shoot a star moving at the typical transverse velocity $v_t \sim 30 \text{ km s}^{-1}$ (De Simone *et al.* 2004), we generally need to carefully extrapolate the future position of the star, by measuring its related parameters. For example, we require the precision $\Delta v_t \sim 0.75 \text{ km s}^{-1}(\Theta/1'')$ for the transverse velocity.

An astrometric mission is an ideal instrument for this measurement. It provides us with five astrometric parameters: the sky position (α, δ) , parallax ϖ and proper motion (μ_α, μ_δ) . All of them are indispensable for our extrapolation.

In 2016, the astrometric mission Gaia released its first data (DR1). Since then, Gaia has brought significant impacts on various fields of astronomy. Its unprecedented precision is expected to also change the shooting problem drastically.

In this paper, using Gaia's latest data release (DR2, Gaia Collaboration *et al.*, 2018), we estimate the number of main-sequence FGK stars suitable for the high precision shooting. These stars would have their habitable zones at $\sim 1 \text{ AU}$. If we observe the systems at the distances of d , the angular separation between the stars and their habitable planets are smaller than $0.1''(d/10\text{pc})^{-1}$. Therefore, we can quite certainly hit the habitable planets once its host star is within our beam of $\Theta \geq 0.1''(d/10\text{pc})^{-1}$. Note that $\sim 20\%$ of the Galactic Sun-like stars could have Earth-size planets in their habitable zones (Petigura *et al.* 2013), but Gaia is unlikely to detect these small planets by astrometric drift (Perryman *et al.* 2014).

We expect that our study would be useful also for SETI, not only for sending signals outward. This is because, it would be advantageous for receivers to inversely assess the potential criteria and strategies of senders at selecting their targets (see e.g. Schelling 1960; Wright 2018; Seto 2019).

Astrometric observation and extrapolation

Here we briefly explain the basic astrometric parameters relevant to our study. On the celestial sphere around a target star, we locally introduce an orthogonal angular coordinate (x_1, x_2) (see Fig. 1). The parallax ϖ is the annual positional modulation on the plane and is determined by the distance d to the star as

$$\varpi = 1.0 \left(\frac{d}{1 \text{ kpc}} \right)^{-1} \text{ mas.} \tag{1}$$

The proper motion (μ_1, μ_2) corresponds to the long-term signature of the time derivatives $\mu_i = dx_i/dt$ ($i = 1, 2$) and is related to the transverse velocity components as

$$v_{t,i} = \mu_i \times d = 4.8 \left(\frac{\mu_i}{1 \text{ mas yr}^{-1}} \right) \left(\frac{d}{1 \text{ kpc}} \right) \text{ km s}^{-1}. \tag{2}$$

We put $v_t \equiv (v_1^2 + v_2^2)^{1/2}$ for the magnitude of the transverse velocity.

Next we discuss the sky position of the target star for our transmission. We introduce a simple Galactic-scale time coordinate t . Also for simplicity, we assume that the astrometric measurement and the shooting are done at the same time $t = 0$ on the Earth. But it is straightforward to incorporate the time interval (realistically $\ll d/c$) between the two operations.

By an astrometric observation, we can basically obtain information of the target at $t = -d/c$ (see Fig. 1). In contrast, our signal

strikes the target around $t = d/c$. Therefore, the following extrapolation is required for the shooting

$$x_{ie} = x_{im} + \frac{2d_m \mu_{im}}{c} \tag{3}$$

$$= x_{im} + \frac{f \mu_{im}}{\varpi_m} \tag{4}$$

(see Fig. 1). Here we use the subscript 'm' for the astrometrically remeasured values (e.g. $x_{im} \equiv x_i(t = -d/c)$) and 'e' for the extrapolated values for the target (e.g. $x_{ie} \equiv x_i(t = d/c)$). If we use the unit [mas yr⁻¹] for μ_{im} and [mas] for (x_{ie}, x_{im}) , we have the numerical value $f = (2 \text{ kpc}/1 \text{ light year}) = 6520$.

As shown in equation (2), the transverse velocity is given by the product $d_m \mu_{im} = v_{t,im}$ and is the primary quantity for adjusting the shooting direction. More specifically, as mentioned earlier and shown in equation (3), the offset angle for the shooting is given by $2(v_{t,im}/c)$. But, in standard astrometric observations, we separately estimate $d_m \propto 1/\varpi_m$ and μ_{im} .

From equation (4), the error for the extrapolated position x_{ie} is given by

$$\delta x_{ie} = \delta x_{im} + f \frac{\delta \mu_{im}}{\varpi_m} - f \frac{\mu_{im} \delta \varpi_m}{\varpi_m^2}. \tag{5}$$

The first term represents the directional error of the target at $t = -d/c$. The second and third terms are those associated with the extrapolation and caused by the errors for the proper motion and the parallax, respectively.

The total number of Gaia DR2 sources is 1 692 919 135 (Brown *et al.*, 2018). Among them, the five astrometric parameters $(\varpi, \alpha, \delta, \mu_{\alpha*}, \mu_\delta)$ are provided for 1 331 090 727 sources, accompanied by the estimation of the associated 5×5 error matrix. Using these data, we can evaluate the 2×2 matrix A for the directional error δx_{ie}

$$A \equiv \begin{pmatrix} \langle \delta x_{1e} \delta x_{1e} \rangle & \langle \delta x_{1e} \delta x_{2e} \rangle \\ \langle \delta x_{1e} \delta x_{2e} \rangle & \langle \delta x_{2e} \delta x_{2e} \rangle \end{pmatrix}. \tag{6}$$

This matrix determines the error ellipse of the extrapolated position (x_{1e}, x_{2e}) in the sky, and we define Δ as the angular size of its long axis (given in terms of the larger eigenvalue of A). If we use an transmitter with a beam opening angle Θ , we should have $\Delta < \Theta$ for hitting the target at a single shot (see Fig. 1).

Our discussions on the uncertainty Δ have been somewhat abstract. Here we make an order-of-magnitude estimation for Δ . For an astrometric observation like Gaia, we have approximate relations for the estimation errors of the related parameters (e.g. $\sigma_\varpi \equiv (\delta \varpi \delta \varpi)^{1/2}$) as

$$\sigma_\varpi \sim \sigma_{x_i} \sim \sigma_{\mu_i} \tag{7}$$

in the units mentioned after equation (4) (Brown *et al.*, 2018). Therefore, in equation (5), the first term is $\sim 10^4(d/1 \text{ kpc})$ times smaller than the second one, and is negligible for our targets at $d = O(1 \text{ kpc})$ discussed in the next section. The ratio between the second and third terms in equation (5) is given by $(v_t/4.8 \text{ km s}^{-1})$ with the transverse velocity v_t . For its typical value $v_t \sim 30 \text{ km s}^{-1}$, equation (5) is dominated by the third term due

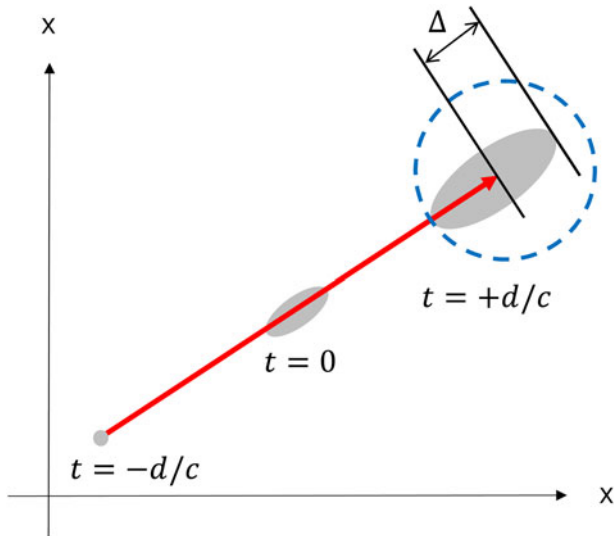


Fig. 1. Prediction of the sky position of a target star in an orthogonal angular coordinate in the celestial sphere. We obtain astrometric information (sky position, parallax and proper motion) of the target at $t = -d/c$ (d : the parallax distance to the target). We then extrapolate the sky position of the target at the hitting epoch $t = d/c$. The directional errors are shown with gray regions. Because of the inaccuracies of the distance and the proper motion, the error size at $t = d/c$ would be much larger than the original size at $t = -d/c$. We define Δ as the angular size of the long axis of the error ellipsoid. To hit the target star at a single shot, we require that Δ is smaller than the beam width Θ of the transmitter indicated by the radius of the dashed blue circle.

to the parallax (distance) error, and we have

$$\Delta \sim 30'' \left(\frac{v_t}{30 \text{ km s}^{-1}} \right) \left(\frac{\sigma_w}{\sigma} \right) \quad (8)$$

$$\sim 3'' \left(\frac{v_t}{30 \text{ km s}^{-1}} \right) \left(\frac{d}{1 \text{ kpc}} \right) \left(\frac{\sigma_w}{0.1 \text{ mas}} \right). \quad (9)$$

In equation (9), we used the characteristic value $\sigma_w \sim 0.1 \text{ mas}$ of Gaia DR2 for a star at G -magnitude $G = 17$ (Brown *et al.*, 2018). In this manner, we can roughly estimate the angular uncertainty $\Delta = O(1'')$ for Gaia DR2 sources at distances $d = O(1) \text{ kpc}$.

So far, we simply fixed the target distance at the observed value $d = d_m$ without considering its time variation. We can, in principle, measure the line-of-sight velocity v_l of the target. But, the line-of-sight velocity v_l introduces an effective change of the transverse velocity only by $O(v_l/c)$ and is totally negligible, compared with the required accuracy level $\sim 0.75 \text{ km s}^{-1}(\Theta/1'')$. Meanwhile the acceleration of the Solar system is estimated to be $O(10 \text{ mm s}^{-1} \text{ yr}^{-1})$ and is dominated by the Galactic centrifugal acceleration (see e.g. Titov and Lambert 2013). If we regard this as the typical secular value for Galactic field stars, the effective velocity shift becomes $0.07 \text{ km s}^{-1}(d/1 \text{ kpc})$ and is not important for the accuracy goal $O(1'')$. In addition, the Galactic potential could be modelled relatively well. Below certain accuracy level, it would be required to deal with additional time-dependent fluctuations of the photon rays such as the relativistic corrections and non-vacuum effects (e.g. scintillation). We leave related studies as our future works.

Table 1. Numbers of our filtered sample and shooting targets

	Filtered sample	Targets $\Delta < 5''$	Targets $\Delta < 1''$	Targets $\Delta < 0.1''$
F	2960592	2320725	888155	8065
G	14224687	9183380	2603038	21441
K	30251412	20315244	4819918	80339
total	47436691	31819349	8311111	109945

Target stars in Gaia DR2

In this section, we examine the actual data set provided in Gaia DR2 and estimate the numbers of stars suitable for our high-precision shooting.

FGK-type stars

Gaia DR2 contains 76 956 778 sources whose effective temperature T_{eff} and radii R are presented, in addition to the five astrometric parameters and their 5×5 noise covariance matrix.² From these sources, we further selected FGK stars potentially hosting habitable planets, by applying the following three filters;

- (i) effective temperature in the three ranges below, F-type: $T_{\text{eff}} \in (6000 \text{ K}, 7500 \text{ K}]$, G-type: $T_{\text{eff}} \in (5200 \text{ K}, 6000 \text{ K}]$ and K-type: $T_{\text{eff}} \in [3700 \text{ K}, 5200 \text{ K}]$,
- (ii) stellar radius: $R \leq 2.0R_{\odot}$ for F-type stars and $R \leq 1.5R_{\odot}$ for GK-type stars,
- (iii) 'Priam flag' value either of the following ones: 0100001, 0100002, 0110001, 0110002, 0120001 and 0120002.

The filter (ii) is for removing evolved stars, and (iii) is for excluding low-quality data (Andrae *et al.* 2018).

After the selection, we obtained 4.7×10^7 stars, as shown in the first column in Table 1. In the following, we call these stars 'filtered sample'. They are anisotropically distributed in the sky with the averaged density $\sim 10^{-4} [\text{arcsecond}^{-2}]$. In Fig. 2 (cyan curve), we present the G -magnitude distribution of our filtered sample. We have a sharp cut-off at $G = 17$ that is mainly determined by the availability of the effective temperature T_{eff} (Brown *et al.*, 2018). In Fig. 3 (cyan curve), we show the cumulative distance distribution for the filtered sample. The median distance is 1.1 kpc and 95% of the sample are within 2.1 kpc.

Note that, for Gaia DR2, all stars are astrometrically analysed as single stars, and some of the filtered sample would be unfavourably affected by the other members of multiple systems. For multiple systems, more elaborate analysis is planned in the next Gaia data release, and we do not discuss the associated effects.

Selecting target stars

Using the prescription based on the 2×2 covariance matrix (6) and the actual data provided in Gaia DR2, we evaluate the angular uncertainty Δ for each of our filtered sample. In Fig. 4 we show the cumulative distribution of Δ . As expected from our

²According to Gaia DR2 site, the uncertainties are underestimated by 7–10% for faint sources with $G > 16$ outside the Galactic plane, and by up to ~ 30 per cent for bright stars with $G < 12$.

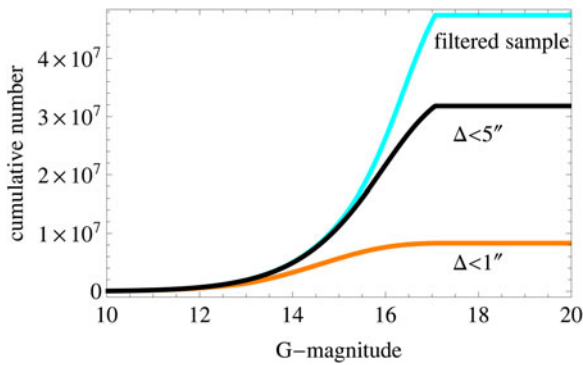


Fig. 2. Cumulative *G*-magnitude distributions of the filtered sample (cyan curve) and of the shooting targets with $\Delta < 5''$ (black curve) and $< 1''$ (orange curve).

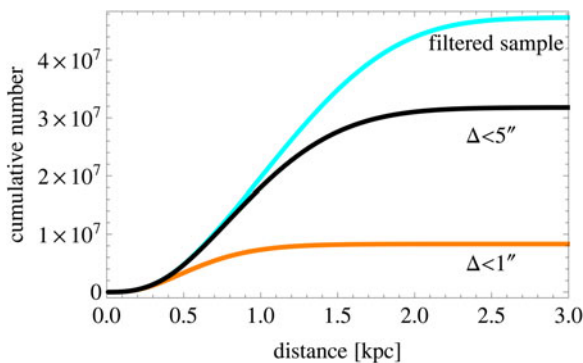


Fig. 3. Cumulative distance distributions of the filtered sample (cyan curve) and of the shooting targets with $\Delta < 5''$ (black curve) and $< 1''$ (orange curve). The median distances are 0.57 and 0.92 kpc for the orange and black curves.

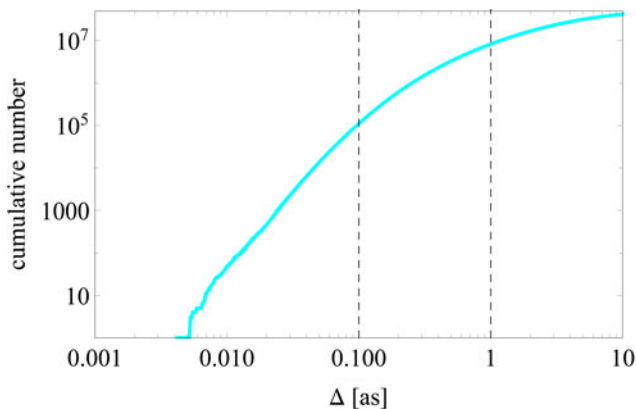


Fig. 4. Cumulative distributions of the uncertainty Δ expected for our filtered sample. The two vertical dashed lines are at $\Delta = 0.1''$ and $1''$.

order-of-magnitude estimation, the characteristic size is $O(1'')$. The best value is $\Delta = 0.0042''$ for a K-star at the distance of 6.7 pc with $G = 7.3$. Given the incompleteness of the Gaia DR2 data at $G < 12$, we should take the lower end of Δ just for a reference as of now.

Now we select our shooting targets by introducing the three fiducial criterion values; $\Delta = 0.1''$, $1.0''$ and $5.0''$, taking into account the specific numerical values quoted in introduction (for $0.1''$ and $1.0''$). The resulting numbers of the targets are summarized in Table I. We have $\Delta < 5''$ for 67% of the filtered sample,

but the fractions decrease to 18% ($\Delta < 1''$) and 0.2% ($\Delta < 0.1''$) for more stringent requirements.

In Figs 2 and 3, we show the distributions of *G*-magnitudes and distances for our targets with $\Delta < 1''$ and $5''$. The median distances for the two criterion values are 0.57 and 0.92 kpc, respectively.

To particularly examine stars hosting confirmed planets, we also utilize the cross match between Gaia DR2 and the NASA Exoplanet Archive. After applying the filters (i)–(iii) to totally 1678 cross-matched stars, we obtain 1259 FGK stars as a subset of our filtered sample. We then evaluate their angular uncertainties Δ and obtain 26 targets with $\Delta < 0.1''$, 782 with $< 1''$ and 1220 with $< 5''$. If we limit our analysis only to host stars of confirmed habitable planets, the subset size is reduced to 60 and we obtain 1 target with $\Delta < 0.1''$, 48 with $< 1''$ and 58 with $< 5''$. Relative to the 4.7×10^7 stars in our original sample, these two subsets have smaller uncertainties Δ .

Positions of the targets

Here we discuss the positions of our shooting targets in the Galaxy. As a representative example, we specifically pick up the subset of the filtered sample whose $1 - \sigma$ error regions of T_{eff} and R are simultaneously within $T_{\text{eff}} \in [5790 \text{ K}, 5890 \text{ K}]$ and $R \in [0.96, 1.04]R_{\odot}$, close to the Solar values. This subset contains 5928 Solar-type stars, and we have 2738 targets for $\Delta < 1''$ and 4847 for $< 5''$. Note that the overall data qualities of this subset are better than our original filtered sample, because of the relatively strong requirements on T_{eff} and R . Accordingly, the target fractions of this subset are higher than those in Table I.

For graphical demonstration, we introduce a Cartesian coordinate (x, y, z) , using the distance d and the Galactic angular coordinate (l, b) as

$$(x, y, z) = d(\cos b \cos l, \cos b \sin l, \sin b). \quad (10)$$

The Galactic centre is at the direction of $+x$ -axis, and the Galactic plane corresponds to the xy -plane. In the upper panel of Fig. 5, we show the projection of the subset sample onto the xy -plane. Most of the orange dots (targets with $\Delta < 1''$) have projected distances less than $\lesssim 1$ kpc, but the black dots (with $1'' < \Delta < 5''$) are distributed over ~ 2.0 kpc. We expect that the observed anisotropy of the stars is mainly due to the Galactic extinction pattern and partially to the sampling pattern of Gaia. If we make a more detailed analysis, we can identify a sparseness of the Solar-type stars in the range $d \lesssim 300$ pc. Given the absolute *G*-magnitude of the Sun $M_G = 4.68$, this is likely to be caused by the incomplete sampling of Gaia for bright stars at $G < 12$.

In the lower panel of Fig. 5, we show the projections of the stars onto the xz -plane. We can see a clear deficit of stars around the x -axis to which the Galactic plane is projected. This reflects the strong extinction towards Galactic plane. In future, some of the inaccessible volume might be explored by the proposed infrared missions such as JASMINE (Gouda 2012) and GaiaNIR (Hobbs 2016). Interestingly, along the x -axis, the boundary of the orange points is not distinctively covered by the black points, unlike the z -axis direction. This indicates that the boundary is mainly determined by the limitation of the temperature estimation, not by the threshold value $\Delta = 1''$.

When the Sun is observed inversely by ETI on a planet around a Solar-type star plotted in Fig. 4, they will record almost the same luminosity, interstellar extinction and transverse velocity as we recorded for the star in Gaia DR2. Therefore, if the ETI have

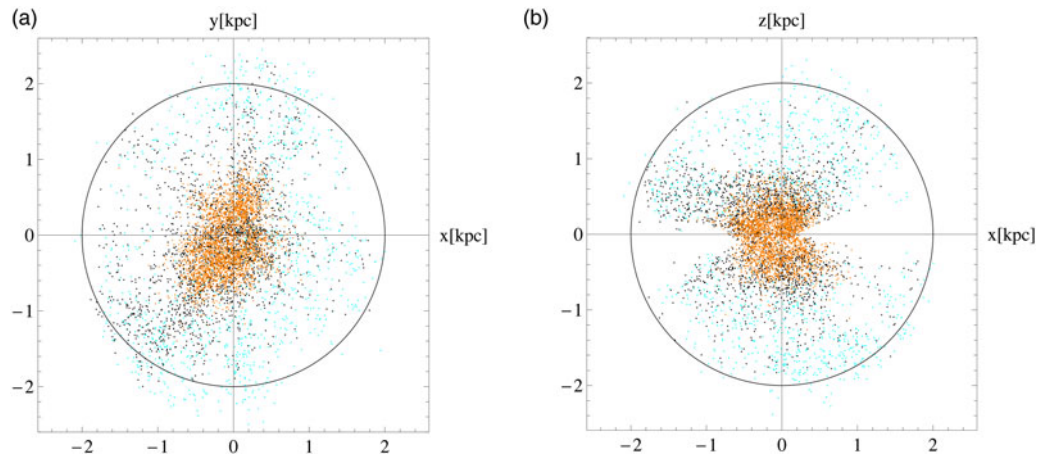


Fig. 5. *Upper panel:* Spatial distribution of 5928 Solar-type stars with $T_{\text{eff}} \sim 5840$ K and $R \sim 1R_{\odot}$. All stars are projected to the Galactic (xy) plane. The orange dots represent 2738 target stars with $\Delta < 1''$ and the black ones show the additional 2109 target stars with $1'' < \Delta < 5''$. The cyan dots are those with $\Delta > 5''$. The Galactic centre is towards the direction of $+x$ -axis. The radius of the black circle is 2 kpc. *Lower panel:* Similarly projected to the xz -plane. The Galactic plane corresponds to the x -axis around which the number of stars are small due to the strong dust extinction.

astrometric mission equivalent to Gaia, they can realize a similar shooting accuracy Δ as we can expect for the star. Here we ignored details such as the source density and orientation of their ecliptic plane, and also assumed that the extinction pattern does not change drastically below the arcmin scale. In this manner, Fig. 4 would be intriguing also from the view point of searching for intentional ETI signatures from Solar-type stars, not just shooting them from the Earth.

Discussions

In this paper, we discussed the prospects of high precision pointing of our transmitters to Galactic habitable planets. For a beam opening angle Θ , we practically want to estimate the future sky position of the host stars with accuracy better than $\Delta < \Theta$. This roughly corresponds to measuring the transverse velocities v_t of the stars with a precision $\delta v_t < 0.75 \text{ km s}^{-1} (\Theta/1'')$ much smaller than the typical value $v_t \sim 30 \text{ km s}^{-1}$.

In the present work, we regarded Gaia as an optimal instrument for our pointing problem. Fully using the astrometric data provided in Gaia DR2, we evaluated the size of the angular uncertainties Δ individually for our filtered sample composed by 4.7×10^7 FGK stars. As summarized in Table I, we have the accuracy $\Delta < 5''$ for 67% of the filtered sample. The fraction decreases to 18% for $\Delta < 1''$.

Until just a few years ago, Hipparcos catalogue was the best available astrometric data. It includes $\sim 2 \times 10^4$ stars whose distances were estimated within $\sim 10\%$ errors. As shown in equation (8), this corresponds to the extrapolation error of at least $\sim 3' (v_t/30 \text{ km s}^{-1})$. With Gaia DR2, our target number is $O(10^7)$ for the accuracy goal $1.0''$ (see Table I), and three orders of magnitude larger than Hipparcos era.

Gaia DR2 is based on the data collected in the first 22 months of observation. Gaia is smoothly operating now, and the mission lifetime could be extended to ~ 2024 , limited by micro-propulsion system fuel.³ With 10 years data, ignoring instrumental degradation, the signal-to-noise ratio of the sources would increase by a factor of 2.3, and the accuracies of the astrometric parameters

would be improved by at least the same factor. The actual improvement is expected to be better than this simple scaling, considering the advantages of the long-term observation both on measuring the proper motion and on reducing the noise correlation between the parallax and other parameters. If we conservatively use the improvement factor 2.3 for Δ in Fig. 4, the numbers of our shooting targets would be 2 and 7 times larger for $\Delta < 1''$ and $< 0.1''$ respectively, compared with Table I. In addition, as we commented earlier, information related to multiple stars would be refined.

In this paper, we studied interstellar communications mainly from the standpoint of a sender. But a sender and a receiver are inextricably linked together, as demonstrated in Fig. 5. In this sense, our results would be suggestive also for SETI-related activities. Here, considering the rapid improvements even of our technology in the past few decades, it would be more productive to gain insights without making strong assumptions on the ETT's technology level.

Acknowledgments. This work has made use of data from the European Space Agency (ESA) mission Gaia, processed by the Gaia Data Processing and Analysis Consortium (DPAC). Funding for the DPAC has been provided by national institutions, in particular the institutions participating in the Gaia Multilateral Agreement. This research was supported by the Munich Institute for Astro- and Particle Physics (MIAPP) which is funded by the Deutsche Forschungsgemeinschaft (DFG, German Research Foundation) under Germany's Excellence Strategy EXC-2094-390783311. We also used the gaia-kepler.fun crossmatch database created by Megan Bedell for the NASA Exoplanet Archive. NS thanks H. Sugiura for his help on python codes. This work was supported by JSPS Kakenhi Grants-in Aid for Scientific Research (Nos. 17K14248, 17H06358, 18H04573, 19K03870).

References

- Andrae R, Fouesneau M, Creevey O, Ordenovic C, Mary N, Burlacu A, Chaoul L, Jean-Antoine-Piccolo A, Kordopatis G, Korn A, Lebreton Y, Panem C, Pichon B, Thévenin F, Walmsley G and Bailer-Jones C (2018) Gaia data release 2. First stellar parameters from Apsis. *Astronomy and Astrophysics* **616**, A8.
- Arnold L (2013) Transmitting signals over interstellar distances: three approaches compared in the context of the Drake equation. *International Journal of Astrobiology* **12**, 212.

³<https://www.cosmos.esa.int/gaia>

- Baum SD, Haqq-Misra JD and Domagal-Goldman SD** (2011) Would contact with extraterrestrials benefit or harm humanity? A scenario analysis. *Acta Astronautica* **68**, 2114.
- Benford J, Benford G and Benford D** (2010) Messaging with cost-optimized interstellar beacons. *Astrobiology* **10**, 475.
- Clark JR and Cahoy K** (2018) Optical detection of lasers with near-term technology at interstellar distances. *The Astrophysical Journal* **867**, 97.
- Cocconi G and Morrison P** (1959) Searching for interstellar communications. *Nature* **184**, 844.
- De Simone R, Wu X and Tremaine S** (2004) The stellar velocity distribution in the solar neighbourhood. *Monthly Notices of the Royal Astronomical Society* **350**, 627.
- Drake FD** (1961) Project ozma. *Physics Today* **14**, 40.
- Gaia Collaboration et al.** (2018) Gaia data release 2. Summary of the contents and survey properties. *Astronomy and Astrophysics* **616**, A1.
- Gajjar V, Siemion A, Croft S, Brzycki B, Burgay M, Carozzi T, Concu R, Czech D, DeBoer D, DeMarines J, Drew J, Enriquez JE, Fawcett J, Gallagher P, Garrett M, Gizani N, Hellbourg G, Holder J, Isaacson H, Kudale S, Lacki B, Lebofsky M, Li D, MacMahon DHE, McCauley J, Melis A, Molinari E, Murphy P, Perrodin D, Pilia M, Price DC, Webb C, Werthimer D, Williams D, Worden P, Zarka P and Zhang YG** (2019) The breakthrough listen search for extraterrestrial intelligence. *Bulletin of the American Astronomical Society* **51**, 223.
- Gouda N** (2012) Infrared space astrometry missions JASMINE missions. *Galactic Archaeology: Near-field Cosmology and the Formation of the Milky Way* **458**, 417.
- Guillochon J and Loeb A** (2015) SETI via leakage from light sails in exoplanetary systems. *The Astrophysical Journal* **811**, L20.
- Hippke M** (2019) Interstellar communication network. I. Overview and assumptions. arXiv e-prints arXiv:1912.02616.
- Hobbs D** (2016) GaiaNIR: Combining optical and Near-Infrared (NIR) capabilities with Time-Delay-Integration (TDI) sensors for a future Gaia-like mission. arXiv e-prints arXiv:1609.07325.
- Horowitz P and Sagan C** (1993) Five years of project META: an all-sky narrow-band radio search for extraterrestrial signals. *The Astrophysical Journal* **415**, 218.
- Perryman M, Hartman J, Bakos GÁ and Lindgren L** (2014) Astrometric exoplanet detection with Gaia. *The Astrophysical Journal* **797**, 14.
- Petigura EA, Howard AW and Marcy GW** (2013) Prevalence of earth-size planets orbiting sun-like stars. *Proceedings of the National Academy of Science* **110**, 19273.
- Schelling TC** (1960) *The Strategy of Conflict*. Cambridge, MA: Harvard University Press.
- Seto N** (2019) Possibility of a coordinated signaling scheme in the galaxy and SETI experiments. *The Astrophysical Journal* **875**, L10.
- Siemion APV, Demorest P, Korpela E, Maddalena RJ, Werthimer D, Cobb J, Howard AW, Langston G, Lebofsky M, Marcy GW and Tarter J** (2013) A 1.1–1.9 GHz SETI survey of the Kepler field. I. A search for narrow-band emission from select targets. *The Astrophysical Journal* **767**, 94.
- Tarter J** (2001) The search for extraterrestrial intelligence (SETI). *Annual Review of Astronomy and Astrophysics* **39**, 511.
- Tarter JC, Agrawal A, Ackermann R, Backus P, Blair SK, Bradford MT, Harp GR, Jordan J, Kilsdonk T, Smolek KE, Richards J, Ross J, Shostak GS and Vakoch D** (2010) SETI turns 50: five decades of progress in the search for extraterrestrial intelligence. *Instruments, Methods, and Missions for Astrobiology XIII* 781902.
- Titov O and Lambert S** (2013) Improved VLBI measurement of the solar system acceleration. *Astronomy and Astrophysics* **559**, A95.
- Vakoch DA** (2016) In defence of METI. *Nature Physics* **12**, 890.
- Wright JT** (2018) Exoplanets and SETI. In *Handbook of Exoplanets*. Cham, Switzerland: Springer International Publishing, p. 186.
- Wright JT, Kanodia S and Lubar E** (2018) How much SETI has been done? Finding needles in the n -dimensional cosmic haystack. *The Astronomical Journal* **156**, 260.
- Zaitsev P** (2010) Messaging to extraterrestrial intelligence. In Shuch HP (ed), *Searching for Extraterrestrial Intelligence*. Chichester, UK: Springer, p. 399.